Detection of a viscoelastic inclusion using spectral attributes of the quasi-stationary seismic surface response

M.-A. Lambert, Spectraseis & ETH Zurich, E.H. Saenger, ETH Zurich & Spectraseis, B. Quintal, ETH Zurich, and S.M. Schmalholz, University of Lausanne*

Summary

This study investigates the feasibility of detecting a viscoelastic inclusion in the subsurface by analyzing the seismic wavefield at the medium's surface. A synthetic quasi-stationary wavefield is generated by random body wave sources at depth. The seismic response at the surface is then analyzed in the frequency domain for lateral variations of two specific spectral attributes. The results show that an inclusion with anomalous attenuation properties can create spectral attribute anomalies in the quasi-stationary background wavefield at the surface. This is even the case in the presence of a shallow low velocity layer. The study provides physical theoretical support for the contention that spectral anomalies in the ambient background wavefield can occur due to anomalously high attenuation properties of hydrocarbon reservoirs.

Introduction

The omnipresent ambient seismic background wavefield in the Earth is permanently modified through interactions with subsurface inhomogeneities. As a consequence, passive ground-motion at the surface may carry valuable information about location, depth, size and seismic properties of underground structures. Conventional analysis techniques based on seismic travel-times are difficult to apply to quasi-stationary ambient ground-motion data because distinct events in the time traces are absent. Interferometry and spectral analysis methods are alternatives and have been successfully applied to a variety of geophysical problems. Nasseri-Moghaddam et al. (2007) used spectral methods to detect and characterize an underground cavity. The cavity caused detectable spectral anomalies because of the seismic velocity contrast to the surrounding rocks. Here, we want to test if a hydrocarbon reservoir can potentially generate similar anomalies in a surface wavefield. Authors have observed abnormally high attenuation, or low quality factor Q, in some reservoirs, often at low seismic frequencies (e.g., Dasgupta and Clark, 1998). Therefore, we investigate the effects of a realistic viscoelastic inclusion on a modeled ambient wave field. The seismic surface response of a quasi-stationary wave field is computed with standard numerical wave propagation simulation. The signals are analyzed in the frequency domain. Specifically, this model provides a feasibility study for detecting the lateral location of an embedded body of anomalous attenuation. The goal of the study is to demonstrate the basic physical plausibility of extracting information on a viscoelastic inclusion by analyzing spectral properties of the surface wavefield. Our simple model may not adequately represent the case of a real reservoir under natural conditions. For example, here we neglect additional complications due to local surface noise sources, complex geology or physical processes that are not captured in our model.

Wavefield modelling

We use a numerical algorithm that solves the 2-D viscoelastic wave equation with the rotated staggered grid finite-difference scheme (Saenger and Shapiro, 2005, and references therein). The 2-D model domain consists of a low-velocity surface layer of 100 m thickness with a uniform half-space underneath. Seismic properties of the media are labeled in Figure 1. The waveforms in Figure 1 show five seconds of vertical component seismograms modeled at 23 stations of the surface receiver array. At the centre of the domain is a 5000 by 250 meter rectangular viscoelastic inclusion. Viscoelasticity is implemented according to equation (4) in Saenger and Shapiro (2005), setting $n = 4$ and using the values $\tilde{Y}_m^{11} = 0.1\, v_P^2\, \rho$, $\tilde{Y}_m^{44} = 0.1\, v_S^2 \rho$ and $\omega_m = 2\pi f_m$, where $f_1 = 1$, $f_2 = 2.7$, $f_3 = 7.4$, $f_4 = 20$. This leads to the frequency dependent attenuation character shown in Figure 2 for both, P- and S-waves. We define Q according to equation (13) in O'Connell and Budianski (1978) as the ratio between the peak kinetic energy density at a given point and its drop over one spatial wavelength. Randomly distributed single point sources are repeatedly and randomly triggered in depths between 3500 m and 4500 m. The source time functions are Ricker wavelets with random central frequencies, acting as body forces in random orientations. The superposition of the signals creates a quasi-stationary band-limited (~1-8 Hz) wavefield, dominated by body waves.

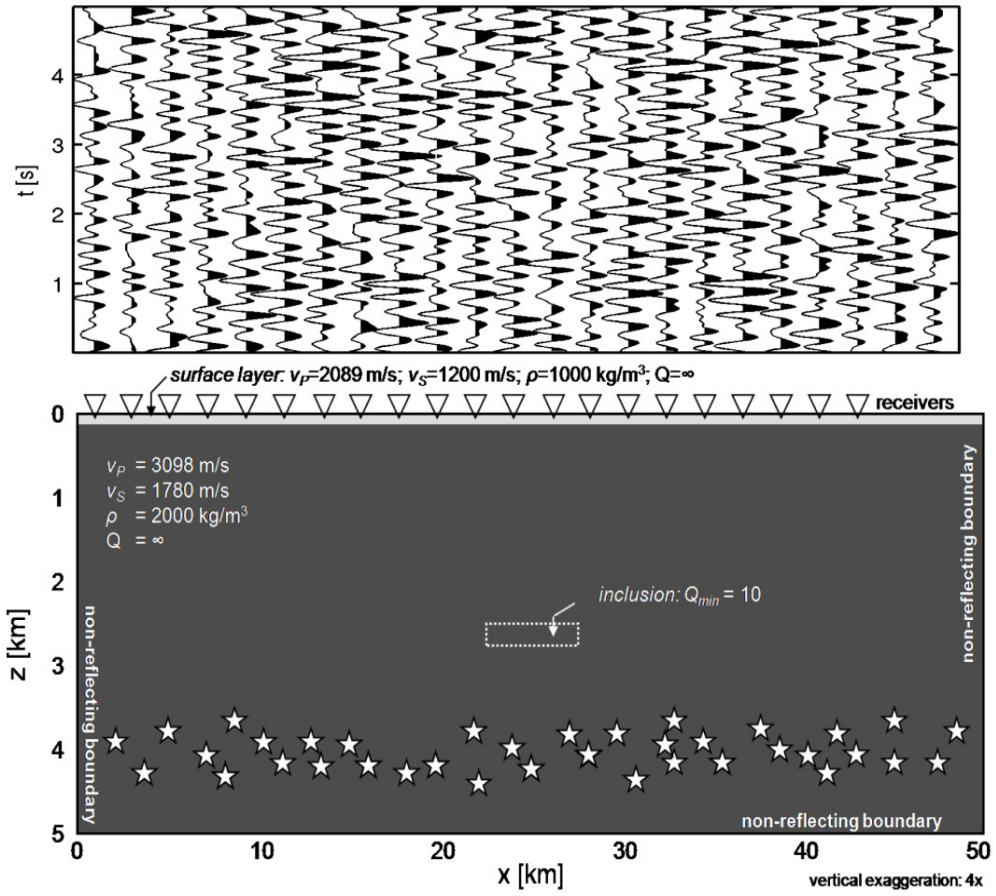

Figure 1: Bottom: Model with a viscoelastic inclusion and a 100 m thick surface layer. Top: Vertical component seismograms at 23 surface stations.

Spectral seismic attributes

Nasseri-Moghaddam et al. (2007) analysed frequency domain parameters of continuous passive seismic surface signals to quantify the energy scattered by a subsurface cavity. We follow a similar data analysis but our target is an embedded body of high attenuation. The modeled particle motion at selected surface locations (receiver array) is transformed into the frequency domain using discrete Fourier transform. The absolute values of the transformed signals yield the amplitude spectra $|X(f)|$ and $|Z(f)|$ for the two principal components of motion (horizontal and vertical). Two specific spectral attributes are calculated from these spectra. The first attribute, A_1, quantifies the wavefield's spectral energy on the vertical component. The vertical spectral energy for a specific receiver r of the total set of receivers S_R is measured as

$$E_V(r) = \sum_{f \in S_F} |Z(r,f)|^2, \quad r \in S_R, \qquad (1)$$

where $|Z(r,f)|$ is the vertical spectral amplitude as a function of receiver r and frequency f. S_F is the set of equidistant discrete frequency values within the interval $[f_1, f_2]$. The energy is normalized by its maximum value across the receiver array to yield attribute A_1:

$$A_1(r) = E_V(r) / \max_{r' \in S_R} E_V(r'). \qquad (2)$$

The second attribute, A_2, is based on an integral value of the ratio between the amplitude spectrum of the vertical and horizontal component of motion (V/H-ratio). This value for receiver r is calculated as

$$\chi(r) = \sum_{f \in S_F} (|Z(r,f)| / |X(r,f)|), \quad r \in S_R. \qquad (3)$$

Attribute A_2 is obtained by normalizing χ by its maximum value across the receiver array:

$$A_2(r) = \chi(r) / \max_{r' \in S_R} \chi(r'). \qquad (4)$$

Detection of a viscoelastic inclusion

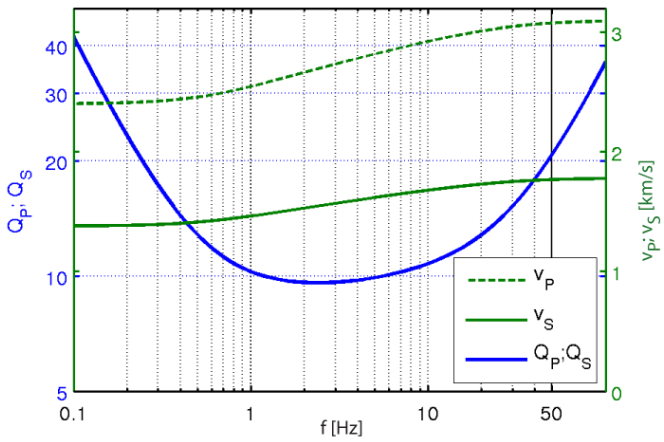

Figure 2: Seismic properties of the viscoelastic inclusion. Velocities of P- and S-waves (v_P, v_S) and corresponding quality factors (Q_P, Q_S) are shown as a function of frequency.

Results

The time-domain data in Figure 1 show a quasi-stationary behaviour in which transient arrivals are not observed. An influence of the inclusion is not obvious in the time domain.

The color plot in Figure 3a displays the vertical component spectral amplitude $|Z(x,f)|$ as a function of frequency f and distance x along the receiver array. The dots in the upper panel of Figure 3a show the values of attribute A_1. The frequency interval $[f_1, f_2] = [1\text{ Hz}, 6\text{ Hz}]$ was chosen for the attribute calculation because it contains the significant part of the modeled energy. The attribute profile (solid line) is smoothed by a running median filter with a window width of 5000 m.

The color plot in Figure 3b shows the spatial spectrogram of the V/H-ratio. The V/H-spectra exhibit characteristic variations with frequency. Reduced values appear around 3 Hz and 9 Hz and enhanced values around 5 Hz. This spectral peak-and-trough pattern is controlled by the S-wave transfer function of the surface layer and is persistent across the whole domain. However, lateral variations are superimposed on this pattern. Increased V/H-ratios around 5 Hz cluster between x = 20 to 30 km above the inclusion. This increase of the V/H-ratio at receivers above the inclusion cannot be explained by effects related to the uniform surface layer. In this model, the only remaining variable is the inclusion at depth. This was tested for a similar model without surface layer (not shown here). The upper panel of Figure 3b shows attribute A_2 which quantifies the lateral variations of the V/H-ratio across the receiver array. The frequency interval $[f_1, f_2] = [4\text{ Hz}, 6\text{ Hz}]$ was chosen to compute attribute A_2 because the strongest lateral variation occurs within this interval.

Figure 3 shows that both attributes are sensitive to the presence of the inclusion at depth. Attribute A_1 exhibits reduced values in the area vertically above the inclusion, although these deviations cannot be considered as significant. However, attribute A_2 shows a clearly confined positive anomaly that is centered within the surface projection of the inclusion.

Synthesis

The relevance of this modelling study with regard to hydrocarbon reservoir characterization depends on the validity of the following two basic assumptions: (i) body waves penetrate reservoirs from below and (ii) reservoirs show high attenuation contrasts to the surrounding. There exist data and studies supporting these assumptions. First, there is evidence of continuous body waves at reservoir depth. For example, Zhang et al. (2009) showed that the ambient background wavefield at low seismic frequencies (0.6 to 2 Hz) is dominated by continuous body wave energy at two sites in California. These body waves originate far away off the coast of California and are excited at the sea floor by wind-generated ocean waves. They propagate on a curved raypath and have penetrated the rock formations at typical reservoir depths in almost vertical direction before they are recorded at the measurement site. Second, high attenuation in hydrocarbon reservoirs has been observed in the field. Dasgupta and Clark (1998), for example, analysed seismic reflection data and found indication for Q as small as 10 for P-waves. One explanation for attenuation in reservoirs at low seismic frequencies is provided by the physical mechanism of wave-induced fluid flow. This mechanism occurs in porous media with partial fluid saturation (White et al., 1975) and/or heterogeneous rock matrix (Pride and Berryman, 2003) and can cause considerable attenuation for both, P- and S-waves (Wenzlau et al., 2010). As suggested by Quintal et al. (2011), the solution for attenuation caused by wave-induced fluid flow in a poroelastic medium can be approximated with an equivalent macroscopic viscoelastic theory. The inclusion in our numerical model is described by this equivalent viscoelastic theory. The parameterization is chosen to yield a minimum Q of about 10, which is low but was shown to be a possible value for hydrocarbon-bearing porous rocks (Dasgupta and Clark, 1998; Quintal et al., 2011).

Conclusions

The results show that an inclusion with anomalous attenuation properties can create spectral attribute anomalies in the quasi-stationary background wavefield at the surface, also in the presence of a shallow low-velocity layer. Data in the time domain is not indicative of the attenuating inclusion. These results provide physical theoretical support for the hypothesis that spectral anomalies in the ambient background wavefield occur due to hydrocarbon reservoirs in the subsurface. This, of course, does not mean that all observed anomalies above reservoirs can be explained by this model. However, demonstrating the physical plausibility of spectral anomalies is an important step and motivates the investigation of more complex/realistic models.

Acknowledgements

E.H. Saenger thanks the DFG (Deutsche Forschungsgemeinschaft) for the support through the Heisenberg Program (SA 996/1-1). M.-A. Lambert thanks Brad Artman for valuable comments and suggestions.

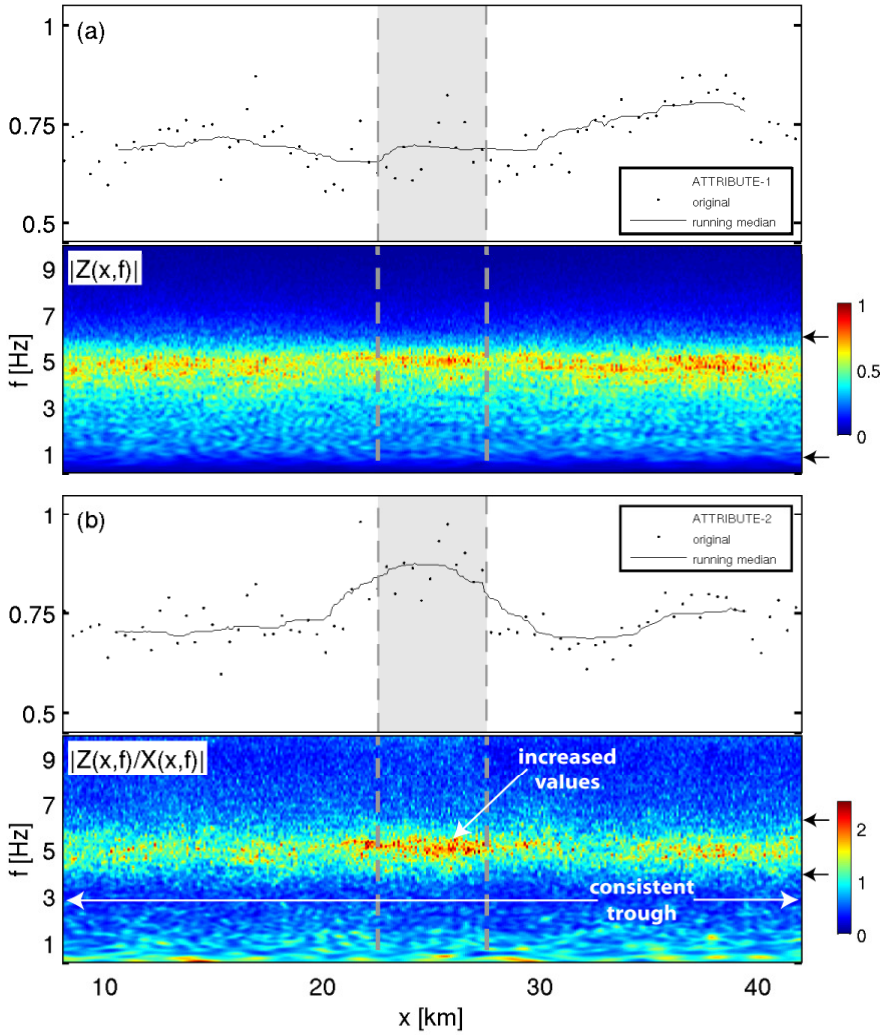

Figure 3: (a) Amplitudes of vertical component versus frequency and distance along the surface (color plot) and profile of attribute A_1. Grey shading indicates the lateral location of the inclusion. (b) V/H-ratio versus frequency and distance (color plot) and profile of attribute A_2.